

On the existence of photoexcited breathers in conducting polymers

S. Tretiak,* A. Piryatinski, A. Saxena, R. L. Martin, and A. R. Bishop

Theoretical Division and Center for Nonlinear Studies, Los Alamos National Laboratory, Los Alamos, New Mexico 87545, USA

(Received 2 August 2004; published 15 December 2004)

Formation and decay mechanisms of photoinduced nonlinear vibronic excitations (“breathers”) in several conjugated polymers are studied using a quantum-chemical excited state molecular dynamics approach. We identify specific coupled vibrational modes responsible for breather excitations and investigate their dependence on chain length. In addition to intermolecular relaxation mechanisms, our calculations show that intramolecular vibrational energy equilibration results in a decay of breathers on a timescale of hundreds of femtoseconds.

DOI: 10.1103/PhysRevB.70.233203

PACS number(s): 78.47.+p, 78.66.Qn, 31.15.Qg, 31.50.Df

Conducting polymers have emerged as important technological materials in device applications based on organic electronics.^{1,2} Compared to the semiconductor devices, the “soft” organic nature of these materials results in a strong coupling of the electronic system to molecular geometries and structure.^{3,4} Thus complex coupled electron-vibrational dynamics strongly affects optoelectronic functionalities of related organic devices. Ultrafast spectroscopies have emerged as a major experimental tool to study short-time electronic dynamics.^{5–7} In particular, the recent advent of lasers with sub-10-fs time resolution has allowed investigators to resolve real-time dynamics on a timescale of a single vibrational period.^{8–10} Signatures of nonlinear vibrational excitations known as breathers (a spatially self-localized bound state of phonons) predicted theoretically in 1984,^{11–13} have been recently observed spectroscopically in polyacetylene.⁸ The breather excitation was found to have a period of 44 fs and an extremely short lifetime of ~ 50 fs. In another recent experiment, time-resolved investigation of vibrational photoexcited dynamics in poly-phenylenevinylene revealed participating nuclear motions similar to those observed in Raman spectra; however, breather signatures were not observed.⁹ Our previous quantum-chemical study revealed formation of a photoexcited self-localized breather vibronic excitation in cis-polyacetylene.¹⁴

Despite the wealth of experimental and theoretical studies, there is no established agreement and understanding as to whether breather excitons are the primary photogenerated excitations and how much they affect ultrafast vibronic dynamics.^{5–9} In this article we use our recently developed excited state molecular dynamics (ESMD) approach⁴ to (i) identify specific features of molecular vibronic structure necessary to produce the photoexcited breather; (ii) explore dissipative processes affecting the breather lifetime; and (iii) investigate breather formation in several typical conjugated polymers to provide a direct connection with the ongoing experimental studies.

We used the Austin Model 1 (AM1) Hamiltonian¹⁵ and the ESMD computational package⁴ to follow photoexcitation adiabatic dynamics on ps timescales for all calculations presented in this article. The ESMD approach calculates the excited state potential energy as $E_e(\mathbf{q}) = E_g(\mathbf{q}) + \Omega(\mathbf{q})$ in the space of nuclear coordinates \mathbf{q} which span the entire

$(3N-6)$ dimensional space, N being the total number of atoms in the molecule. Here, $\Omega(\mathbf{q})$ is an electronic transition frequency to the lowest $1B_u$ (band-gap) state of the photoexcited molecule. The program uses numerical derivatives of $E_e(\mathbf{q})$ with respect to each nuclear coordinate q_i to calculate forces and subsequently to step along the excited state hypersurface using these gradients. A standard Verlet molecular dynamics algorithm¹⁶ has been used for propagation of the Newtonian equations of motion. All computations start from the optimal molecular geometry where the potential energy $E_g(\mathbf{q})$ is minimal. The simulations can be performed along all ($i=1, \dots, 3N-6$) or selected nuclear degrees of freedom q_i . If no dissipative processes are included, the total molecular energy $E_e(\mathbf{q})$ is conserved. Subsequent analysis of the photoexcited trajectory of $\Omega(\mathbf{q}, t)$ in the Fourier space allows us to identify periods of participating vibrational motions. A similar approach has been used in the analysis of time-resolved transient absorption spectra in recent experiments.^{8–10} Inclusion of an artificial dissipative force into the ESMD equations of motion allows us to determine the minimum of the excited state potential energy surface $E_e(\mathbf{q})$ corresponding to the relaxed geometry.

To understand the formation of photoexcited breathers we start with an analysis of the dynamics of the band-gap excited state in the cis-polyacetylene oligomer shown in Fig. 1. This molecule is sufficiently long (120 carbon atoms) to mimic the infinite chain limit.¹⁷ Displacements Δ shown in Fig. 1 immediately enable us to identify several nearly degenerate vibrational normal modes strongly coupled to the electronic excitation with a period of ~ 18 fs. These correspond to C=C stretching motions which self-localize to form the breather excitation (see below). The mode q_0 with the largest displacement has the lowest frequency and corresponds to a nearly uniform displacement of carbons along the chain as schematically shown in Fig. 1 (top). Higher lying C=C vibrations have an increasing number of nodes along the chain (e.g., mode q_2 has two nodes). These states can be interpreted as phonons with momenta $k=2\pi n/L$ (n being the number of nodes and L is the length of the molecule) and form a band in the limit of the infinite chain length. Another vibrational band corresponding to C—C single bond stretching motions has smaller displacement and does not lead to breather excitation.

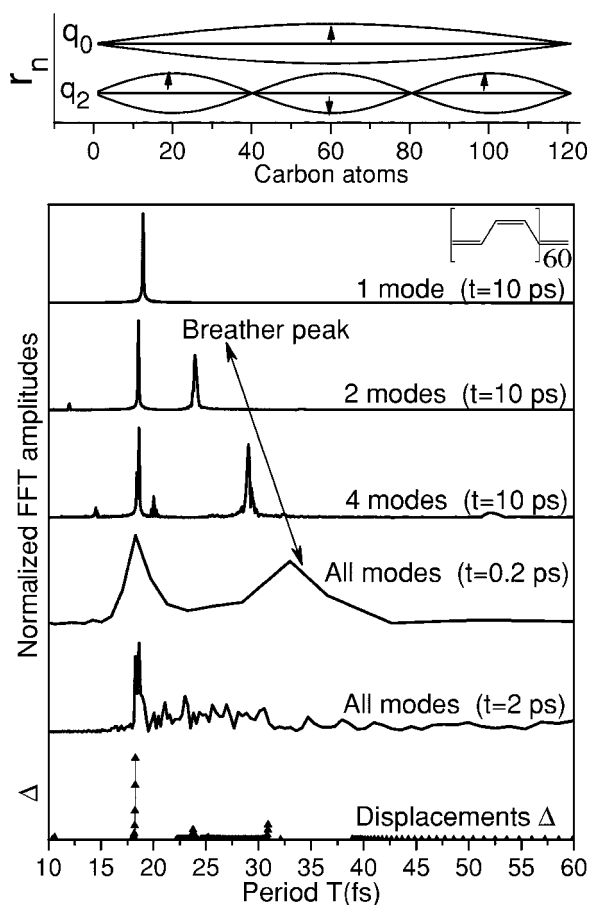


FIG. 1. Top panel: displacements of the backbone atoms in C=C stretching vibrational modes forming a phonon band (shown are modes corresponding to $k=0$ and $k=2$ phonon momenta). Bottom panel: normalized Fourier spectra of the excited state transition energy $\Omega(t)$ trajectories (top five plots) and amplitudes of dimensionless displacements Δ_i (stick spectrum) along normal modes (bottom plot) in *cis*-polyacetylene [*(cis-PA)*₆₀ shown in the inset]. Amplitudes of Δ_i reflect the difference between the excited state and the ground state optimal geometries along the vibrational modes (with harmonic periods T_i) and typically show the extent of coupling of the electronic degrees of freedom to specific nuclear motions (Ref. 18).

When we artificially freeze all vibrational motion except a single q_0 normal mode, as expected the photoexcited dynamics is completely harmonic with a single fundamental frequency (with time period of 18 fs) appearing in the Fourier spectrum (10 ps trajectory has been used to obtain power spectra in Fig. 1). The dynamics along two vibrational coordinates q_0 and q_2 already shows, in addition to the fundamental period at 18.3 fs, a second component at 24 fs which is not an overtone of the fundamental frequency. This peak is a signature of the breather excitation appearing as a nonlinear mixing of vibrational modes due to anharmonicities and complex coupling to the electronic degrees of freedom. Compared to the harmonic single mode dynamics, the two-mode dynamical trajectory (not shown) samples most of the energetically allowed phase space and shows signatures of intermittent spatiotemporal chaos. Four-mode dynamics (phonons with momenta $k=0, 2, 4,$ and 6) increases the

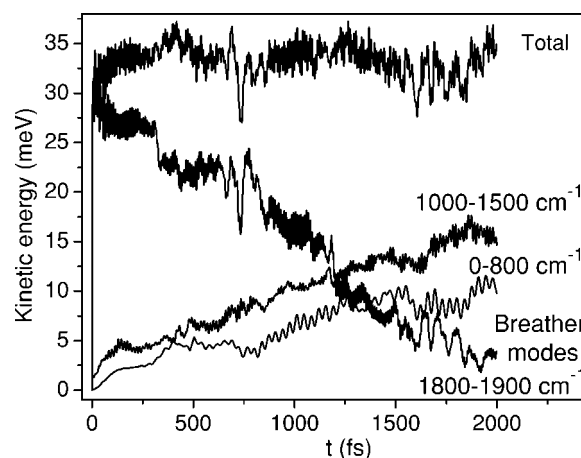


FIG. 2. Variation of the vibrational kinetic energy along the photoexcited trajectory in *(cis-PA)*₆₀. Averaging over 20 fs has been used to smooth fast oscillations.

breather period to 30 fs. Thus a set of quasidegenerate nuclear modes strongly coupled to the electronic system allows for breather formation. Finally, complete *short time* (200 fs trajectory) dynamics along all $3N-6$ vibrational degrees of freedom identifies a strong breather peak at 34 fs.

However, the power spectrum of $3N-6$ mode dynamics of a long (2 ps) trajectory shows no breather signatures (Fig. 1). To illustrate this breather decay, in Fig. 2 we display the averaged kinetic energy along the photoexcited trajectory. The total vibrational energy is approximately constant during the dynamics and corresponds to the excess of electronic energy due to vertical excitation. The variation of the kinetic energy indicates that the energy is exchanged between electronic and vibrational degrees of freedom. Just after photoexcitation, only vibrational modes in the 1800–1900 cm^{-1} spectral region are activated. These correspond to the “breather modes” strongly coupled to the electronic system. Gradually this energy transfers to other vibrational modes due to vibrational anharmonicities and weak coupling to the electronic excitation. A similar behavior is observed in other conjugated polymers (not shown). Thus we observe equilibration of vibrational energy among all nuclear degrees of freedom. This intramolecular relaxation leads to the decay of breather excitation on a timescale less than 500 fs. Intermolecular dissipative processes might reduce breather lifetime even further due to interchain interactions and scattering of phonons on the defects. This readily explains the very short breather lifetime of 50 fs observed in the experiment.⁸

Next we calculate photoexcited dynamics in several *cis*-polyacetylene oligomers with different sizes to explore the dependence of breather excitation on chain length. The respective Fourier spectra of photoexcited trajectories are shown in Fig. 3. We observe a reduction in the amplitude and a shorter period of the breather peak with a decrease in chain length. Subsequently this peak disappears in short chains ($n < 20$ repeat units). This trend can be rationalized by examining the band structure of the underlying breather vibrational modes. As the splitting between states grows due to the finite molecular size (see $\Delta\omega$ in Fig. 3), the vibrational mode mixing becomes less efficient resulting in the reduction of the breather amplitude.

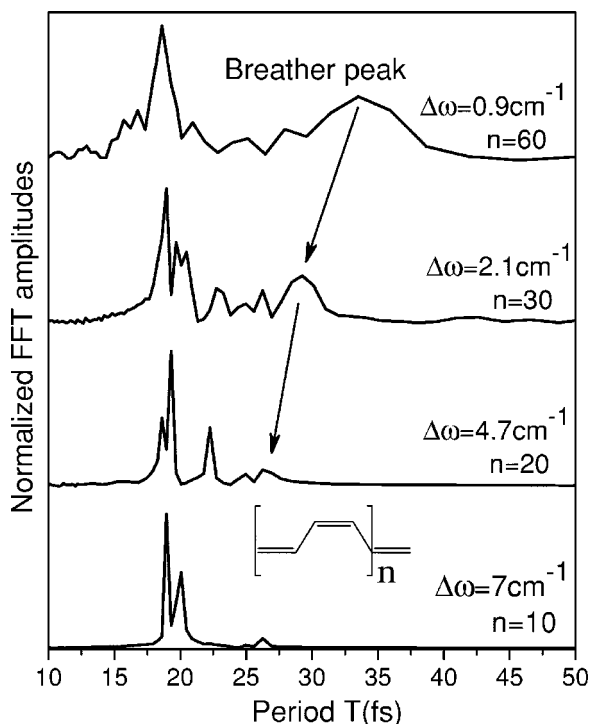


FIG. 3. Size dependence of the intensity of the breather peak in Fourier spectra of 400 fs photoexcited trajectory in cis-polyacetylene. $\Delta\omega$ is a splitting between frequencies of q_0 and q_2 vibrational modes.

Finally, we study the appearance of the breather excitation in several technologically important polymers. To treat all molecules on the same basis, we constructed oligomers of the same length (~ 100 Å) for cis-polyacetylene [(cis-PA)₄₈], polyphenylenevinylene (PPV)₁₆, polyfluorene [(PF)₆], and polythiophene [(PT)₁₄] shown in the insets of Fig. 4. Computation of longer chains is not practical due to the increased computational effort [e.g., (PF)₆ has already more than 700 atomic basis functions in the valence space]. Compared to polyacetylene, the richer geometric structure of the other polymers leads to the appearance of several vibrational bands in the displacement spectra (Fig. 4) which are strongly coupled to the electronic system. For example, two displaced bands in PPV are attributed to C=C stretch and quinoidal motion of the aromatic rings. To investigate breather formation, we then ran constrained photoexcited dynamics for 10 ps along normal modes strongly coupled to the electronic system (ten modes from two vibrational bands in cis-PA and PPV, and 15 modes from four vibrational bands in PF and PT).

As expected, a strong breather peak shows up in polyacetylene (Fig. 4). A weaker breather signature shifted to 27 fs is observed in PPV. Here the C=C stretch couples to aromatic ring motion. Since C=C groups and rings do not couple directly to each other, neither produces the breather by itself. Constrained dynamics along vibrations from the only one of these bands (not shown) does not show breather signatures. Therefore, compared to cis-PA, breather excitation in PPV appears due to mixing of vibrations from the different bands. This leads to a faster breather decay on an

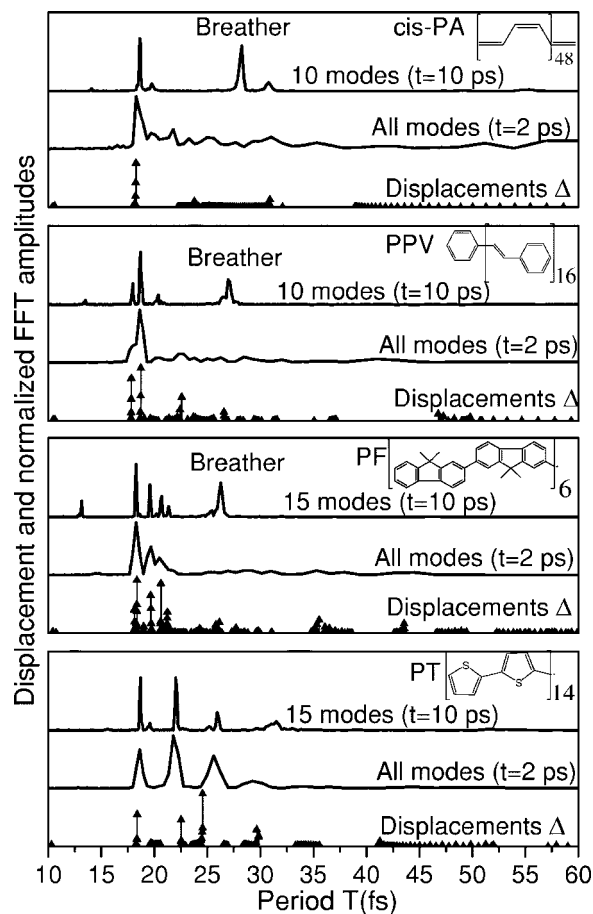


FIG. 4. Analysis of photoexcited dynamics in conjugated polymers. Structures of oligomers with ~ 100 Å length are shown in the insets. Plotted are normalized Fourier spectra of photoexcited trajectories and displacements.

~ 100 fs timescale due to intramolecular vibrational energy redistribution in the dynamics including all $3N-6$ vibrational coordinates (the breather peak can be barely identified in the respective Fourier spectrum of the short-time trajectories, not shown). This has probably prevented an identification of the breather in PPV with ultrafast spectroscopic probes.⁹

We observe the breather excitation in PF to be weaker than in cis-PA but stronger than in PPV. Similar to PPV, it forms due to mixing of vibrations from three different bands and decays on an ~ 200 fs timescale if all normal coordinates are included in the dynamics (Fig. 4). Substantial spectral density of weakly coupled nuclear modes at the breather frequency is another reason for a fast breather decay in PPV and PF (compare displacements in Figs. 1 and 4). We cannot identify breather signatures in PT since significant spectral separation among participating vibrational bands prevents an efficient mixing. Possible weak breather peak can be seen in the constrained dynamics (Fig. 4). As expected, long-time (2 ps) dynamics in all oligomers including all vibrational degrees of freedom only reveals signatures of the dominant fundamental frequencies (Fig. 4). To summarize, the excess of photoexcitation energy (roughly the difference between vertical and 0-0 transition energies) is able to create a strong breather excitation in cis-PA and weaker breathers in PPV and

PF. We also note that an artificial increase of the vibrational energy (heating) of the relevant normal modes in the numerical simulations leads to strong breather appearance in all polymers.

In conclusion, we have numerically investigated the appearance of breathers by vertical photoexcitation in several conducting polymers. Nonlinear mixing of several (two or more) vibrational modes strongly coupled to the electronic degrees of freedom leads to the breather formation. A strong breather mode is observed in cis-polyacetylene as a result of interaction among vibrations within the *same* phonon band. Weaker breathers in polyphenylenevinylene and polyfluorene appear due to coupling of vibrations among several *different* phonon bands. Polythiophene does not show any breather signatures due to vertical photoexcitation. In every case, the breather excitation undergoes a fast decay (~ 500 fs in cis-PA, ~ 100 fs in PPV, and ~ 200 fs in PF) due to intramolecular vibrational energy equilibration. Such fast decay agrees

with recent ultrafast spectroscopic data (e.g., breather decay in polyacetylene within 50 fs⁸ and vibrational dephasing of the excited states in PPV with a time constant of ~ 300 fs⁹). Intermolecular interactions and phonon energy leakage through the boundaries of conjugated segments (defects) may reduce breather lifetime even further.¹⁴ Nonlinear vibrational excitations such as breathers are thus an important feature of short-time (~ 100 – 500 fs) photoexcited dynamics in conjugated materials. A similar analysis can be applied to other molecular systems to identify signatures of nonlinear vibronic excitations.

The research at LANL is supported by the Center for Nonlinear Studies (CNLS) and the LDRD Program of the U.S. Department of Energy. This support is gratefully acknowledged. The authors thank A. P. Shreve for useful discussions.

*Electronic address: serg@cnls.lanl.gov

¹A. J. Heeger, Rev. Mod. Phys. **73**, 681 (2001).

²R. H. Friend, R. W. Gymer, A. B. Holmes, J. H. Burroughes, R. N. Marks, C. Taliani, D. D. C. Bradley, D. A. Dos Santos, J. L. Bredas, M. Logdlund, and W. R. Salaneck, Nature (London) **397**, 121 (1999).

³J. L. Brédas, J. Cornil, D. Beljonne, D. A. dos Santos, and Z. Shuai, Acc. Chem. Res. **32**, 267 (1999).

⁴S. Tretiak, A. Saxena, R. L. Martin, and A. R. Bishop, Phys. Rev. Lett. **89**, 097402 (2002).

⁵R. Lécuyer, J. Berrehar, C. Lapersonne-Meyer, and M. Schott, Phys. Rev. Lett. **80**, 4068 (1998).

⁶G. S. Kanner, Z. V. Vardeny, G. Lanzani, and L. X. Zheng, Synth. Met. **116**, 71 (2001).

⁷K. M. Gaab and C. J. Bardeen, J. Phys. Chem. B **108**, 4619 (2004).

⁸S. Adachi, V. M. Kobryanskii, and T. Kobayashi, Phys. Rev. Lett. **89**, 027401 (2002).

⁹G. Lanzani, G. Cerullo, C. Brabec, and N. S. Sariciftci, Phys.

Rev. Lett. **90**, 047402 (2003).

¹⁰S. L. Dexheimer, A. D. VanPelt, J. A. Brozik, and B. I. Swanson, Phys. Rev. Lett. **84**, 4425 (2000).

¹¹A. R. Bishop, D. K. Campbell, P. S. Lomdahl, B. Horovitz, and S. R. Phillpot, Phys. Rev. Lett. **52**, 671 (1984).

¹²S. R. Phillpot, A. R. Bishop, and B. Horovitz, Phys. Rev. B **40**, 1839 (1989).

¹³J. I. Takimoto and M. Sasai, Phys. Rev. B **39**, 8511 (1989).

¹⁴S. Tretiak, A. Saxena, R. L. Martin, and A. R. Bishop, Proc. Natl. Acad. Sci. U.S.A. **100**, 2185 (2003).

¹⁵M. J. S. Dewar, E. G. Zoebisch, E. F. Healy, and J. J. P. Stewart, J. Am. Chem. Soc. **107**, 3902 (1985).

¹⁶M. P. Allen and D. J. Tildesley, *Computer Simulation of Liquids* (Clarendon, Oxford, 1987).

¹⁷S. Tretiak and S. Mukamel, Chem. Rev. (Washington, D.C.) **102**, 3171 (2002).

¹⁸A. B. Myers, Acc. Chem. Res. **30**, 519 (1997).